FAKULTA STROJNÍ
ZÁPADOČESKÉ
UNIVERZITY
V PLZNI

EXPERIMENTAL RESEARCH OF TURBINE FLOW PATH
SVOČ – FST 2019

Ing. Marek Klimko,
University of West Bohemia in Pilsen,
Univerzitni 8, 301 00 Pilsen
Czech Republic

ABSTRACT

The paper describes the research activities on the VT-400 test air turbine. Device VT-400 is part of the experimental research on Power System Engineering Department. The paper provides basic information about the current state of the test rig, describes the used measurement techniques and methods for data processing and evaluation.

KEYWORDS

Axial turbine, flow path, experimental turbine, measurement.

INTRODUCTION

A research of turbine flow path is very important in order to increase an efficiency and reliability of turbomachines. Generally, it can be preceded in several ways. The most suitable would be if the research were performed on real turbines in operation. However, options of such experiments are very limited, usually the consist of extended guaranteed measurements providing basic performance data. The second option is represented by measurements on experimental test rigs in laboratories. A construction of those turbines provides the possibility of investigating flow fields in various operation modes by using special probes. The results can be compared to the design regimes. However, and the problem may arise later on when solving and portability of those results on real machines, which is necessary. [1]
This paper deals with experimental work on an experimental air turbine VT-400, which is part of research activities at the Department of Power System Engineering.

BASIC DESCRIPTION OF EXPERIMENTAL DEVICE

Device VT-400 is a single stage air turbine located at the compressor suction. The turbine stage is a model of the high pressure steam turbine part in the 1:2 dimension. This layout provides an easy access to the turbine and measurement points. A scheme of the test rig is shown in Figure 1.

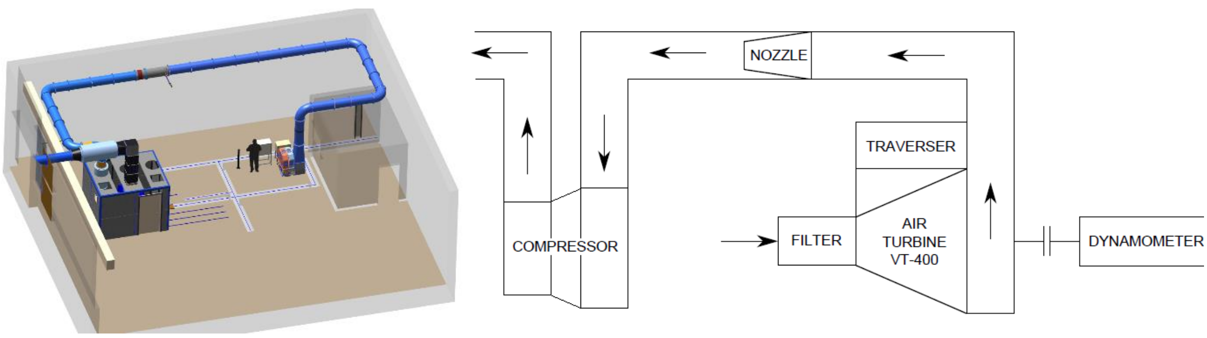

Figure 1: Schematic representation of the test rig

Before the air enters the turbine there is a filter through which the air is sucked from the laboratory. The turbine is equipped with a traversing device that includes two pneumatic five-hole probes, for wake traversing behind the nozzle and the bucket row. The power generated by the blades is obtained by calculating the RPM and torque. Values are measured using a dynamometer, which is connected to the turbine rotor by a flexible coupling. Mass flow is determined by a nozzle located in the pipeline that connects the turbine to the fan. It is an axial-radial fan with an available pressure drop of 12 500 Pa. Due to the pressure losses generated in the flow of the whole line, the pressure gradient available for the turbine stage is reduced to 10 000 Pa. [2]

TESTED GEOMETRIES

Measured turbine stages was designed by Doosan Skoda Power company. At present, three different reaction turbine stages are available. The geometric parameters are summarized in the following Table 1. These three turbine stages contain one common nozzle blade row. Only the bucket wheel with different reaction is changed.

Table 1: Geometrical parameters of tested stages

NOZZLE			**BUCKET**		
Root diameter [mm]	D_P^{NZL}	400	Root diameter [mm]	D_P^{BCK}	400
Blade length [mm]	L^{NZL}	45.5	Blade length [mm]	L^{BCK}	47
Chord [mm]	c^{NZL}	22.5	**Output relative velocity angles [°]**		
Output absolute velocity angle [°]	α_1	14.5°	Low reaction - LR (25%)	β_2^{LR}	19.9°
			Mid reaction - MR (35%)	β_2^{MR}	19°
			Full reaction - FR (50%)	β_2^{FR}	14.5°

MEASUREMENT TECHNIQUES

Measurement is divided into two typical tasks. The first task is to measure the so-called "integral characteristics" (turbine stage performance) evaluated from static pressure taps (Figure 2). The flow path is equipped with a number of static pressure taps in all measured planes (0 to 5). These planes are shown in the following figure.

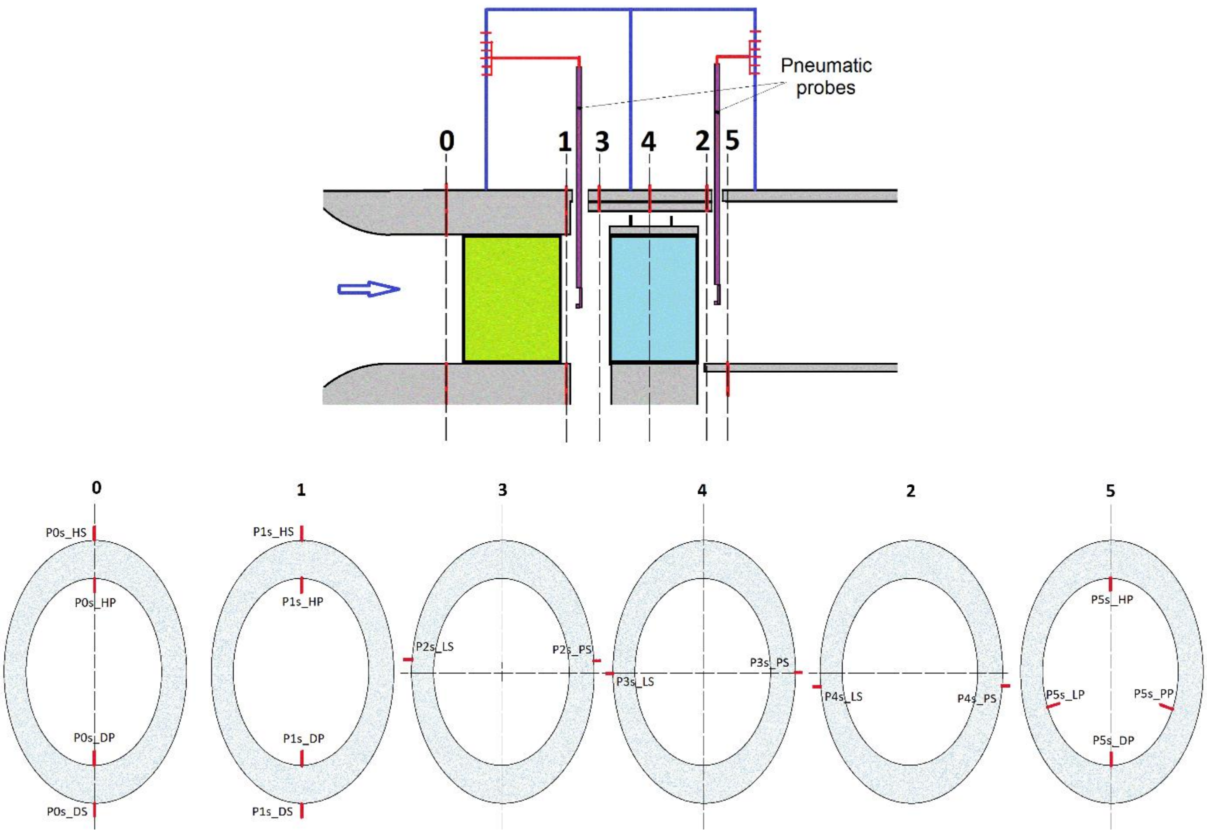

Figure 2: Turbine flow path with measured points

The second type of measurement is the traversing of the flow fields behind the nozzle and bucket blade rows. There are two five-hole pneumatic probes that are indicated on Figure 2. Generally, we distinguish the stage efficiency defined on the basis of the "*total-to-total*" (T-T) and "*total-to-static*" (T-S), which is determined from the total input and static output states (see equations 1 and Figure 3).

TURBINE STAGE PERFORMANCE

The theoretical thermodynamic turbine stage efficiency is characterized by the mechanical work ratio of 1 kg working medium to the energy supplied to the stage [3].

$$\eta_{T-T}^{ST} = \frac{H^{ST}}{H_{iz}^{ST} + \frac{c_0^2}{2} - \frac{c_2^2}{2}} \quad ; \quad \eta_{T-S}^{ST} = \frac{H^{ST}}{H_{iz}^{ST} + \frac{c_0^2}{2}} \tag{1}$$

These relations for calculating the efficiencies are evident from the following "*h-s*" flow diagram (Figure 3) of the working medium expansion in the turbine stage.

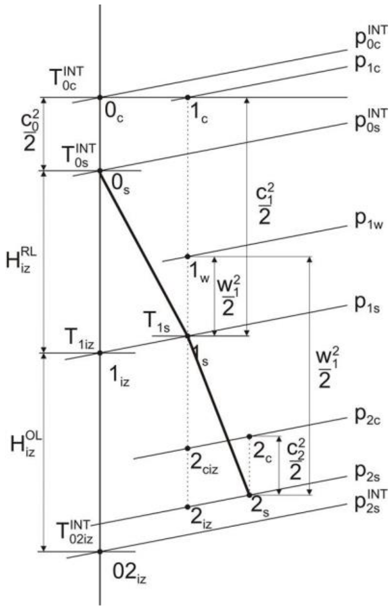

Figure 3: "h-s" diagram of turbine stage expansion [3]

In turbine practise, the dependence of turbine stage efficiency on u/c_f parameters is very often used. This dependence characterizes so-called turbine stage performance.
For illustration in the following graphs (Figure 4) are shown dependencies of turbine stage efficiency on dimensionless parameter u/c_f. This is the ratio of the circumferential velocity u (at the centre profile of the rotor blade) to the isentropic (fictive) expansion speed c_f.

$$c_f = \sqrt{2 \cdot \left(H_{iz}^{RL} + H_{iz}^{OL} + \frac{c_0^2}{2}\right)} = \sqrt{2 \cdot H_0} \tag{2}$$

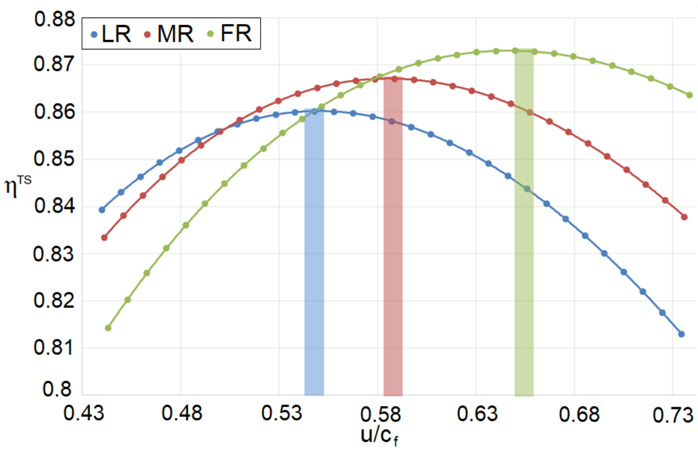

Figure 4: Comparison of turbine stage efficiency dependencies with optimal u/c_f values

These graphs represent a simple 1D analysis of the turbine stage for the mid blade profile and for different reaction values listed in Table 1. More detailed information can be found in the publication [3]. These dependencies serve only for a basic idea because the boundary conditions were very simplified. It serves only to better understand the effects of individual parameters.

Measurement and evaluation methodology

For evaluating a turbine stage characteristic is necessary to collect information about RPM, torque, pressure, temperature and intake air humidity. An overview of all these values needed for the following evaluation is given in Table 2.

Table 2: Measured data

Measured parameter	Symbol	Unit
Turbine RPM (dynamometer)	n	1/min
Torque (dynamometer)	Mk	Nm
Ambient pressure (digital barometer)	p_B	Pa
Ambient temperature (digital barometer)	t_{0c}	°C
Relative humidity (digital barometer)	ϕ_0	%
Static pressures (planes 0, 1, 4, 5)	$p_{0s} \dots p_{5s}$	Pa
Temperature behind the nozzle	t_{cl}	°C
Input and output nozzle static pressures	p_{cl1}, p_{cl2}	Pa

Turbine stage efficiency is calculated according to the relations (1), where:

$$H^{ST} = \frac{P + \boldsymbol{P_{loss}}}{\dot{\boldsymbol{m}}} \quad ; \quad P = M_K \cdot \omega = M_K \cdot \frac{\pi \cdot n}{30} \tag{3}$$

Parameter *P* is dynamometer power that is calculated from RPM and torque.

Equation (3) contains parameter P_{loss} (power dissipation). This parameter is understood as a power needed to cover the frictional energy losses in bearings and other rotating parts. The power dissipation is taken from the power generated by the rotor blades, so it is important to make a professional estimation and include it into the evaluation process.

The value of the power dissipation was determined by a combination of measurements and also by the power loss relations provided by the bearings manufacturer. First, the bearing losses loaded only with radial force were determined experimentally at selected turbine RPM range (0 – 3000). Subsequently, the value of the power dissipation caused by the different axial forces that was obtained from the bearing manufacturer´s relations were added to the dependencies. The resulting dependence is plotted on the following graph (Figure 5). Thus, it can be seen that the magnitude of the power dissipation is a function of the RPM and the axial force acting on the rotor.

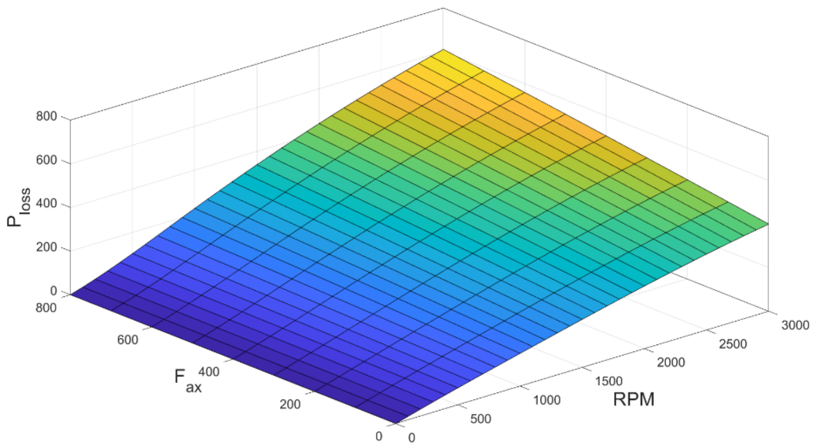

Figure 5: Power loss distribution

Another unknown variable in equation (3) it the mass flow parameter $\dot{m}$. An ASME standard nozzle is used to mass flow measure. For its determination we need to know the static pressures behind and in front of the nozzle and temperature.

The mass flow is evaluated from the general Bernoulli equation for isentropic and stationary flow. In the resulting relation (4) occurs c_q, which is the flow coefficient dependent on Reynolds number.

$$\dot{m} = \frac{c_q}{\sqrt{1-\left(\frac{S_2}{S_1}\right)^2}} \cdot S_2 \cdot \sqrt{2\rho_1(p_1-p_2)} \cdot \frac{\sqrt{1-\left(\frac{S_2}{S_1}\right)^2}}{\sqrt{1-\left(\frac{S_2}{S_1}\right)^2 \cdot \left(\frac{p_2}{p_1}\right)^{\frac{2}{\kappa}}}} \cdot \frac{\left(\frac{p_2}{p_1}\right)^{\frac{1}{\kappa}} \cdot \sqrt{\frac{\kappa \cdot p_1}{\kappa - 1}\left[1-\left(\frac{p_2}{p_1}\right)^{\frac{\kappa-1}{\kappa}}\right]}}{\sqrt{p_1-p_2}} \tag{4}$$

In the evaluation script, this coefficient is automatically calculated according to the current Reynolds number and the whole calculation is based on CSN 5167-3 standard.
The calculated mass flow is the total flow that flows through the measurement loop. Due to air leakage through the shroud sealing, the resulting mass flow must be corrected.

$$\dot{m}_{corr} = \dot{m} - \dot{m}_L \tag{5}$$

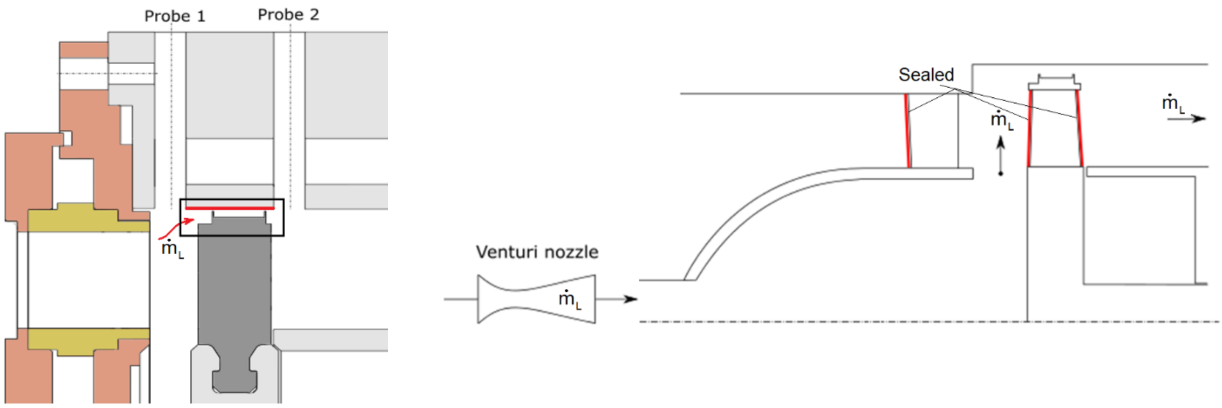

Figure 6: Flow path with marked leakage over the shroud sealing (left) and adjusted loop for tip leakage flow calibration (right) [2]

The tip leakage flow is calculated using an empirical formula by "Samoljovich" and compared with the calibration test on our turbine. The nozzle and bucket row blading was sealed and the mass flow was measured by additional Venturi nozzle located in front of the loop (Figure 6 right).
In the following Figure 7 is a comparison of the calculation ("Samojlovich") and the experiment.

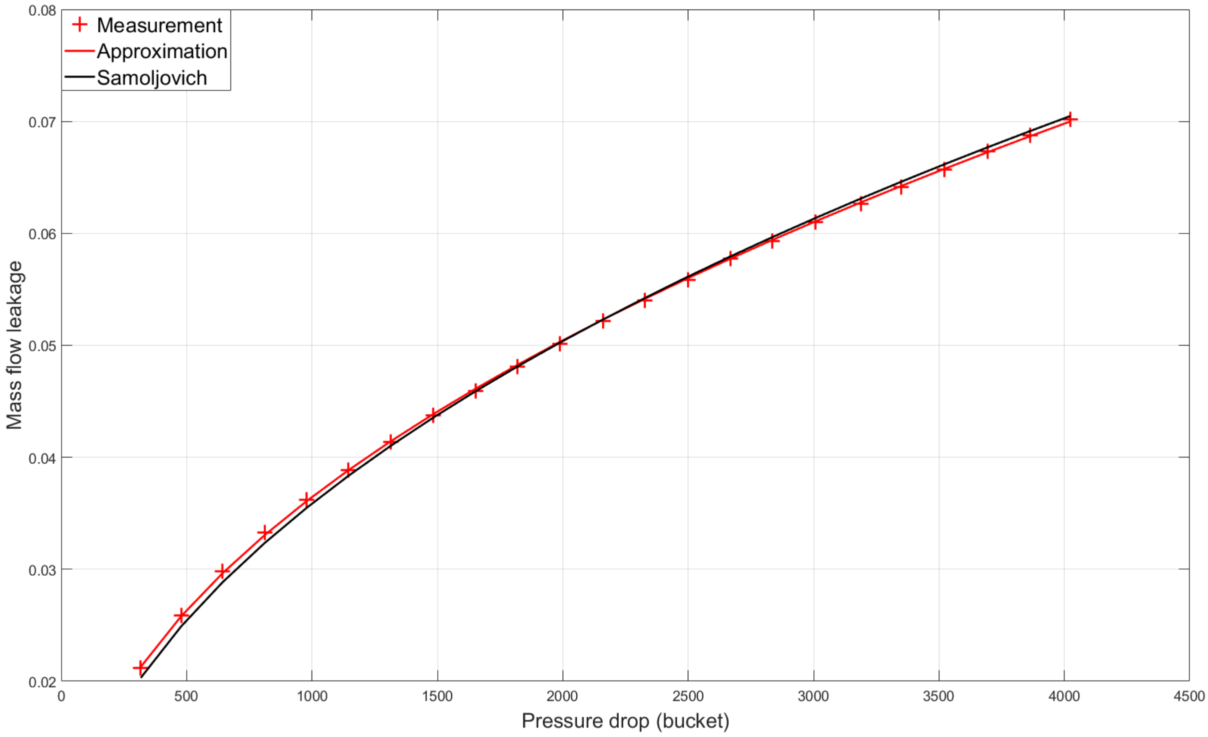

Figure 7: Tip leakage flow calibration

Mass flow correction from the tip leakage flow calibration was entered into the evaluation process.
The conclusion of the evaluation is the individual points expansion line calculation and the plotting turbine stage efficiency depending on the speed ratio u/c_f (Figure 8). The results correspond to the design assumptions.

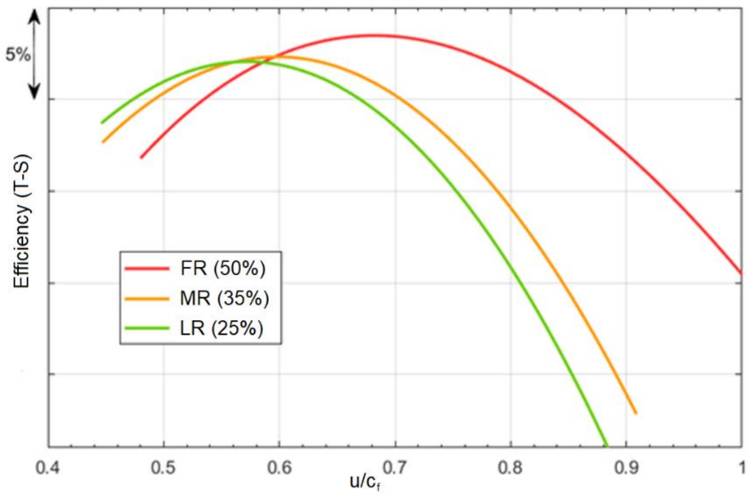

Figure 8: Turbine stage efficiency measurement [4]

UNCERTAINTY QUANTIFICATION ANALYSIS

Background theory

Uncertainty analysis expresses the interval at which the real value of a measurand is located with a certain probability. It is based on the relations for standard uncertainties analysis for indirect measurement because the output parameter Y is a known function of the input parameters $(X_1, X_2, \ldots, X_m)$. These input variables can be directly measured or their estimates, uncertainties, and covariance are detected from other sources.

$$Y = f(X_1, X_2, \ldots, X_m) \tag{6}$$

The estimate y of the output variable Y is then determined from equation (7)

$$y = f(x_1, x_2, \dots, x_m) \tag{7}$$

where x_1, x_2, ..., x_m are estimates of input variables X_1, X_2, ..., X_m. For uncorrelated estimates x_1, x_2, ..., x_m, the estimation uncertainty y of Y is determined as follows.

$$u^2(y) = \sum_{i=1}^{m} A_i^2 u^2(x_i) \tag{8}$$

For sensitive coefficient (A_i) applies:

$$A_i = \frac{\partial(X_1, X_2, \dots, X_m)}{\partial X_i}\bigg|_{X_1=x_1,\dots,X_m=x_m} \tag{9}$$

Measuring apparatus errors

Two *Scanivalve DSA 3217/16Px* pressure transducers and one *Intelligent Pressure Scanner 9000* were used for pressure measurement. A summary of the ranges and accuracy of each channel is described in the Table 3.

Table 3: Transducers ranges and accuracy

Sensor pressure range	Static accuracy (% F.S.)
± 10 inch H_2O (2.5 kPa)	± 20%
± 1; ± 2.5 psid	± .12%
± 5 to 500 psid	± .05%
± 501 to 750 psid	±.08%

The ambient air properties in the lab are scanned using the *VAISALA PTU 300* multipurpose digital barometer for barometric pressure, relative humidity and temperature measurements.

Table 4: Barometer ranges and accuracy

Barometric pressure		Relative humidity (RH)		Temperature	
Range	500…1100 hPa	Range	0…100% RH	Range	-40…+60°C
Linearity	± 0.05 hPa	Accuracy (+15…+25°C)	± 1% RH (0…90% RH) ± 1.7% RH (90…100% RH)	Accuracy (+20°C)	± 0.2 °C
Hysteresis	± 0.03 hPa	Calibration uncertainty (+20°C)	± 0.6 % RH (0…40% RH) ± 1% RH (40…97% RH)		
Total accuracy (-40…+60°C)	± 0.15 hPa				

In addition to the ambient air temperature, the temperature in the outlet pipe behind the turbine, which enters the calculation of the mass flow, is also measured. The *PT-100* sensor is used for the measurement.

Table 5: PT-100 ranges and accuracy

Range	-50…400°C
Accuracy	< 0.05°C
Linearity	< 0.05 % full scale

A 50 kW dynamometer is used for rotational speed and torque measurement. Torque measurement error is 0.5% from full scale.

Determining the uncertainty of the turbine stage efficiency

To calculate the uncertainty of turbine stage efficiency, it is necessary to adjust the relation for efficiency to include all measured parameters from which the sensitive coefficients are determined.

$$\eta_{TT} = f(M_k, n, \underbrace{p_{cl1}, p_{cl2}, T_2}_{\dot{m}_{corr}}, T_{0s}, p_{0s}, p_{2s}) \tag{10}$$

$$\eta_{TT} = \frac{\sqrt{\sigma_3}\sqrt{p_{\mathrm{cl1}} - p_{\mathrm{cl2}}}\left(\frac{M_k \cdot n \cdot \pi}{30} + P_{loss}\right)}{S_{cl2} \cdot c_q \left(\frac{p_{\mathrm{cl2}}}{p_1}\right)^{\frac{1}{\kappa}} \left\{ T_{0s} c_p \left[\left(\frac{p_{2s}}{p_{0s}}\right)^{\frac{\kappa-1}{\kappa}} - 1\right] - \frac{R_v^2 \cdot S_{cl2}^2 \cdot T_{0s}^2 \cdot c_q^2 \cdot \sigma_4 \sigma_1 \cdot \frac{\sigma_2}{R_v T_2}}{4 S_1^2 \cdot p_{0s}^2 \cdot \sigma_3 (p_{\mathrm{cl1}} - p_{\mathrm{cl2}})} + \frac{S_{cl2}^2 \cdot c_q^2 \cdot p_{4s}^2 \cdot \sigma_4 \sigma_1 \cdot \frac{\sigma_2}{R_v T_2}}{4 R_v^2 \cdot S_2^2 \cdot T_{0s}^2 \cdot \sigma_3 \cdot (p_{\mathrm{cl1}} - p_{\mathrm{cl2}}) \left(\frac{p_{2s}}{p_{0s}}\right)^{2 \cdot \left(\frac{\kappa-1}{\kappa}\right)}} \right\} \cdot \sqrt{\sigma_5} \sqrt{\frac{\sigma_2}{R_v T_2}}} \tag{11}$$

Individual sensitivity coefficients are quite complex mathematical relations that because of the space requirements are not specified. Their numerical values after substitution are given in the balance Table 6.

Table 6: Balance table

Measurand	Estimate	Standard uncertainty	Sensitive coefficients	Uncertainty contribution	Uncertainty
Mk	27.13	0.25	0.0323	0.008075	6.52056E-05
n	2302.311	2	3.80E-04	0.0007604	5.78208E-07
p_{cl1}	89756.62	13.8	-2.78E-04	-0.0038364	1.4718E-05
p_{cl2}	88117.3	13.8	2.73E-04	0.003764778	1.41736E-05
T_2	295.024	0.4	1.50E-03	0.0006	0.00000036
T_{0s}	298.863	0.4	-0.0035	-0.0014	0.00000196
p_{0s}	96811.78	13.8	-1.63E-04	-0.00225423	5.08155E-06
p_{2s}	91312.01	13.8	1.74E-04	2.40E-03	5.78301E-06
Overall uncertainty					0.010385563

Torque measurement has the largest proportion of the resulting uncertainty (60%). In the future, it is considered to replace dynamometer with a more accurate torque flange.

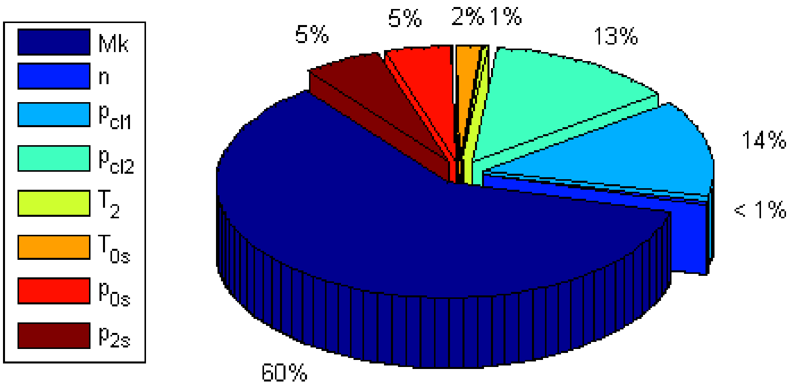

Figure 9: Diagram of partial uncertainties

CONCLUSION

The paper briefly describes a part of the research activity on the VT-400 air turbine. A measuring loop including the tested turbine blade geometry designed by the Doosan Skoda Power company has been described. The paper deals with the turbine stage integral characteristic evaluation. There was also briefly described data measurement process and measurement uncertainty methodology. In addition to the mentioned type of measurement, wake traversing behind the nozzle and bucket using five-hole probe is also realized. However, a description of this issue would exceed the paper allowed range.

ACKNOWLEDGEMENT

The presented research is supported by the student project SGS-2014-070 (Increasing the efficiency. reliability and durability of power system devices 3).

REFERENCES

A Chapter in the magazine or in the Collective Publication:

[1] Zitek. P. – Klimko. M. – Noga T.: *Experimental air turbine.* AIP Conference Proceedings. **1768** (8). 2016. p. 1-8. DOI: 10.1063/1.4963048.

[2] Skach. R. – Uher. J. – Milcak. P. – Zitek. P. – Klimko.M.: *Construction modification of an experimental air turbine.* EPJ Web of Conference, will be published.

[3] Klimko.M.: *Theoretical study of turbine stage characteristics in off-design conditions.* AIP Conference Proceedings. **2047** (9). 2018. p. 1-9. DOI: 10.1063/1.5081641.

[4] Uher. J. – Milcak. P. – Skach. R. – Fenderl. D. – Zitek. P. – Klimko. M..: *Experimental and numerical evaluation of losses from turbine hub clearance flow.* ASME TurboExpo. 2019., will be published

A research reports:

[5] Klimko. M.: *Uncertainty estimation of the VT-400 full reaction turbine stage circumferential efficiency*. Technical report. 2018.

[6] Klimko. M.: *1D turbine stage calculation under off-design conditions.* Technical report. 2018.

[7] Zitek. P. – Uher. P. - Klimko. M.: *Experimentální porovnání plně a středně reakčního turbínového stupně.* Technical report. 2017.